Electronic Supplementary Information

Polyhydroxyalkanoate derived hydrogen bond donors for synthesis of new Deep Eutectic Solvents

Authors

Katarzyna Haraźna[1], Karolina Walas[2], Patrycja Urbańska[2], Tomasz Witko[3], Wojciech Snoch[1], Agnieszka Siemek[1], Barbara Jachimska[1], Marcel Krzan[1], Bogna D. Napruszewska[1], Małgorzata Witko[1], Szczepan Bednarz[2], Maciej Guzik[1,*]

1 Jerzy Haber Institute of Catalysis and Surface Chemistry Polish Academy of Sciences, Niezapominajek 8, 30-239 Krakow, Poland

2 Cracow University of Technology, Department of Biotechnology and Physical Chemistry, Warszawska 24, 31-155, Krakow, Poland

3 Faculty of Physics, Astronomy and Applied Computer Science, Jagiellonian University, Łojasiewicza 11, 30-348, Kraków, Poland

* correspondence to: Maciej Guzik, ncguzik@cyfronet.pl

Keywords

Deep Eutectic Solvents; (*R*)-3-hydroxyacids; polyhydroxyalkanoate; choline chloride; 1-ethyl-3-methylimidazole chloride; tributylmethylammonium chloride

Abstract

Bacterial polyesters are well known group of polymers with excellent biocompability and biodegrability properties. They are also renewable source of wide array of enantiopure (*R*)-3-hydroxycarboxylic acids. In this study, a series of ternary Deep Eutectic Solvents (DES) systems were prepared using mixture of microorganisms-derived (*R*)-3-hydroxynonanoic and (*R*)-3-hydroxyheptanoic acids in a molar ratio of 7:3 as hydrogen bonds donors (HBD) and selected quaternary ammonium salts as hydrogen bonds acceptors (HBA) namely, choline, 1-ethyl-3-methylimidazolium and tributylmethylammonium chlorides. For comparison, DESs based on aliphatic carboxylic acids analogues, i.e. nonanoic and heptanoic acids were also studied. The systems were characterized by ^{1}H NMR and FT-IR techniques and formation of hydrogen bonds between HBD and HBA was proved. The thermal properties including melting temperatures and thermal stabilities as well as polarity, wetting properties were determined by DSC, TGA, Nile Red method and dynamic contact angle methods, respectively. The viscosity and density were measured over a temperature range of 30-60 ^{o}C. Cytotoxicity and biodegradation studies were conducted revealing non-toxic character of choline based DES. The ability of the DESs to dissolve lignin was also evaluated. The results demonstrated new area of application of bacterial polyesters for synthesis of novel biobased solvents.

Graphical abstract

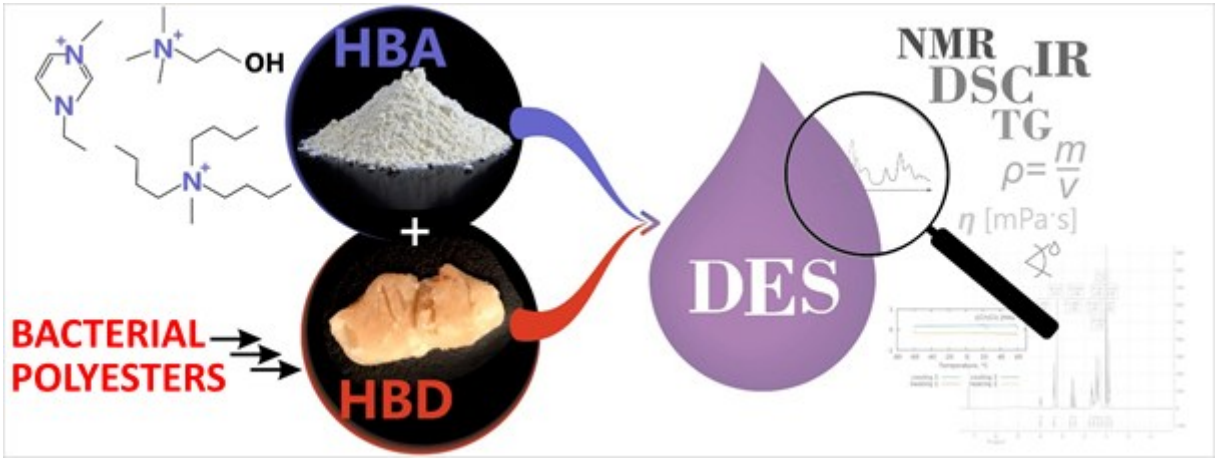

Supporting Information

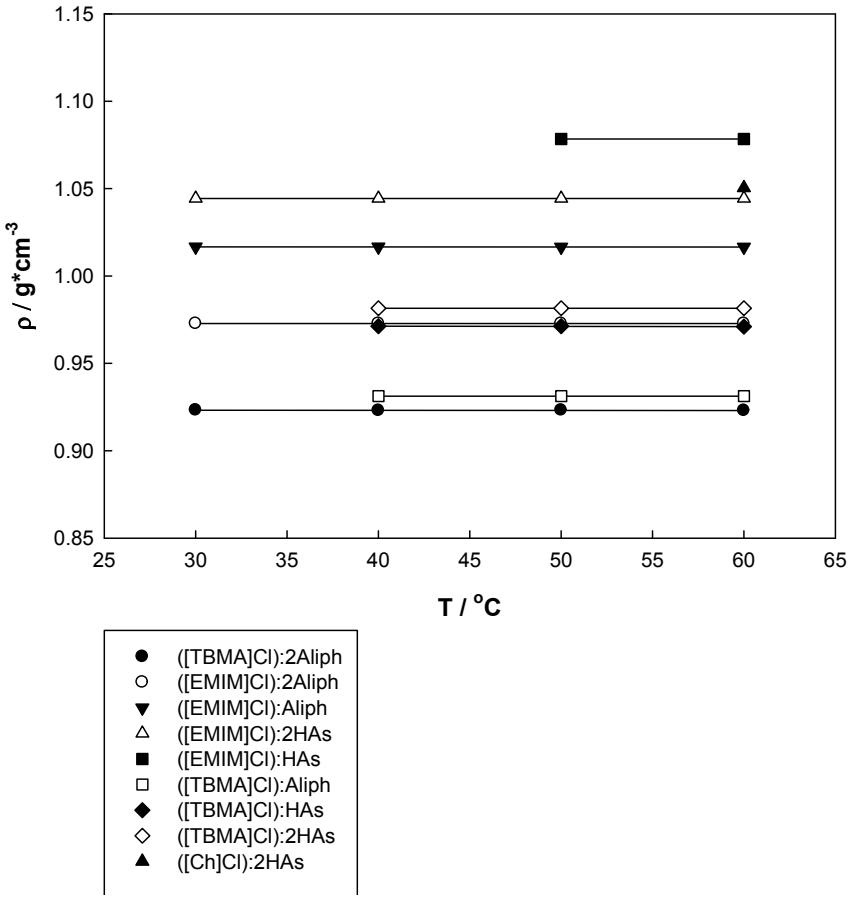

Figure S1. Density measurements obtained for DESs

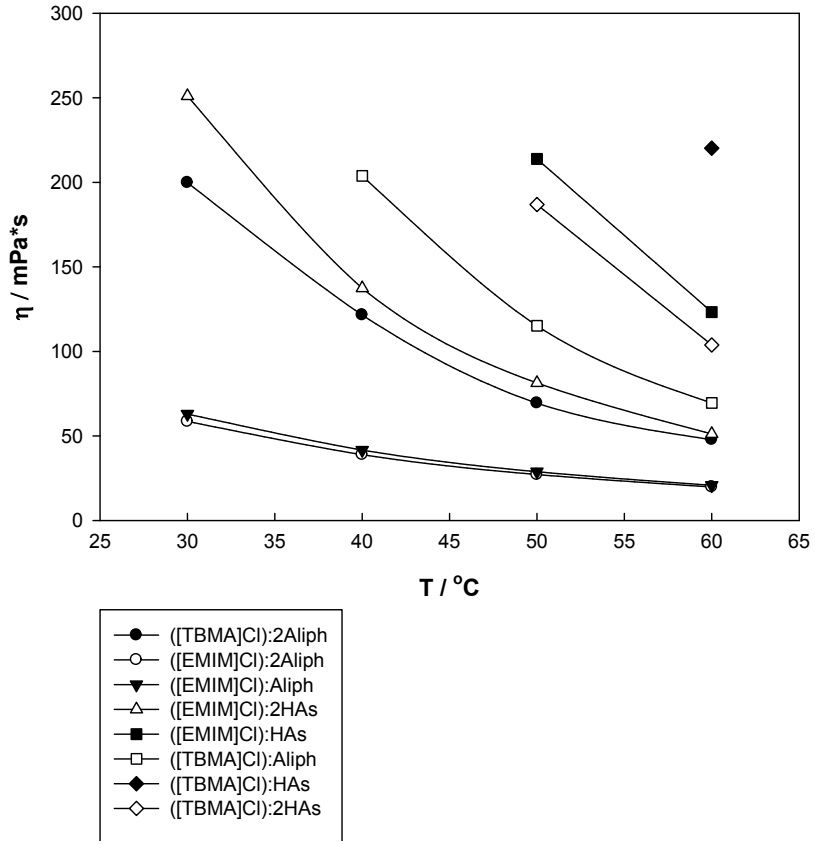

Figure S2. Kinetic viscosity measurements obtained for DESs

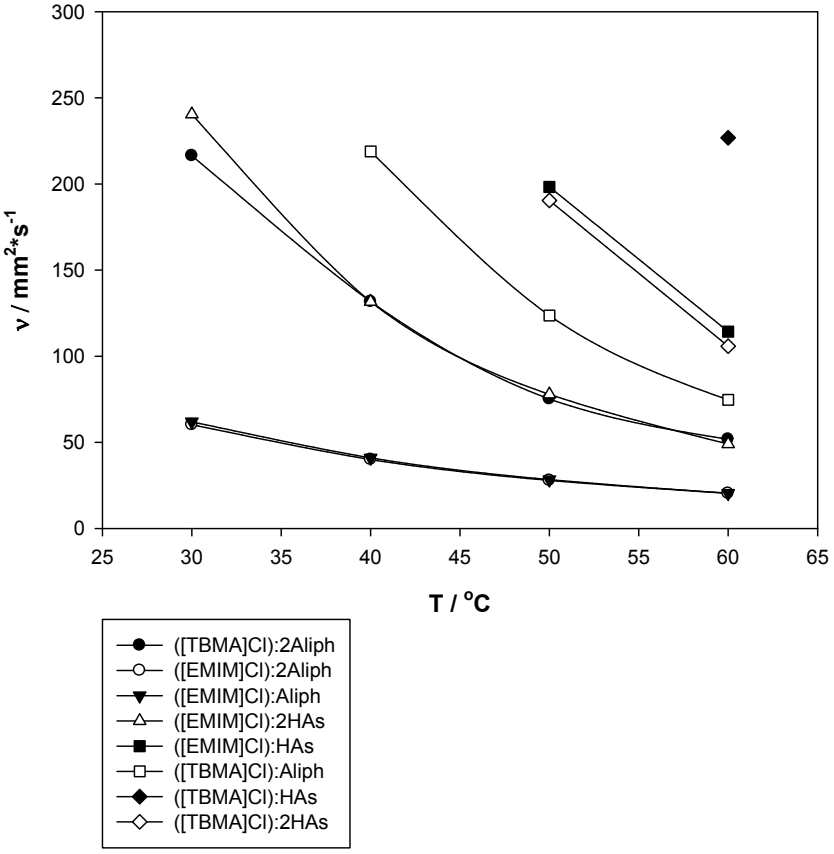

Figure S3. Dynamic viscosity measurements obtained for DESs

^{1}H NMR spectra

Choline chloride ([Ch]Cl)

^{1}H NMR (300 MHz, Deuterium Oxide) δ 4.00 – 3.89 (m, 2H, c), 3.45 – 3.36 (m, 2H, b), 3.09 (s, 9H, a).

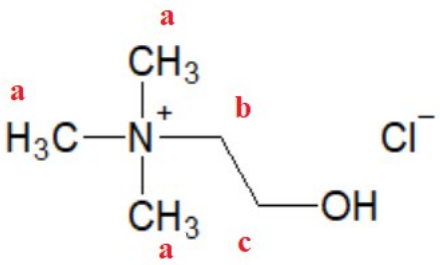

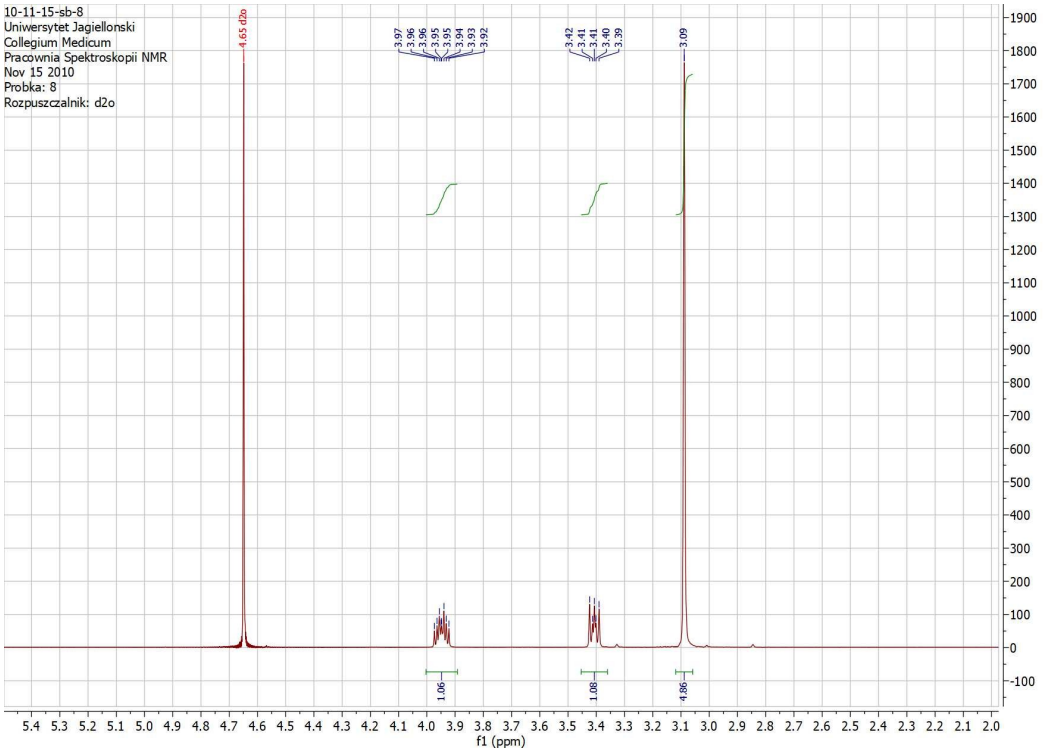

Figure S4. NMR spectrum of choline chloride ([Ch]Cl)

Tributylmethylammonium chloride ([TBMA]Cl)

^{1}H NMR (300 MHz, Chloroform-*d*) δ 3.48 – 3.36 (m, 6H, d), 3.28 (s, 3H, e), 1.72 – 1.55 (m, 6H, c), 1.40 (h, *J* = 7.3 Hz, 6H, b), 0.96 (t, *J* = 7.3 Hz, 9H, a).

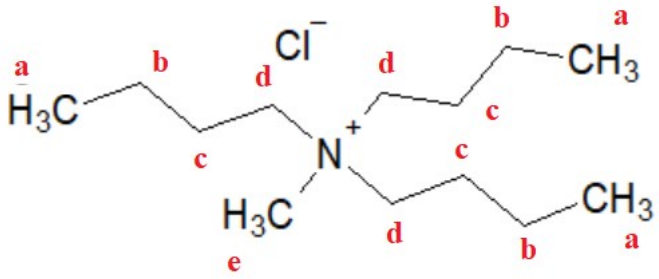

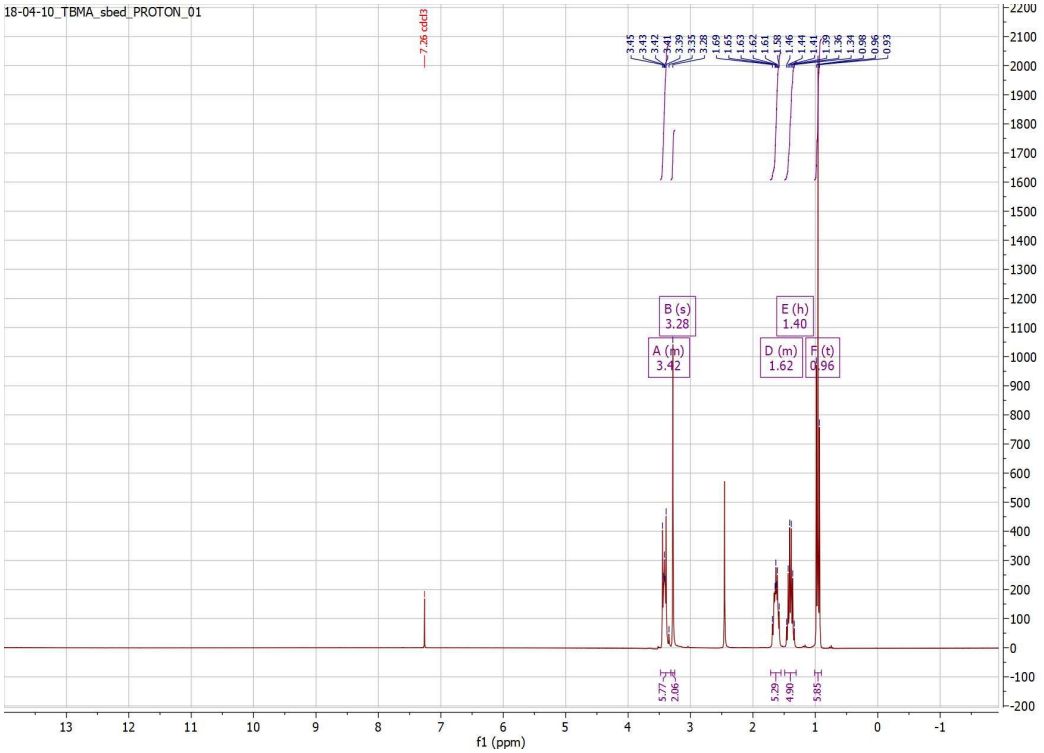

Figure S5. NMR spectrum of tributylmethylammonium chloride ([TBMA]Cl)

1-Ethyl-3-methylimidazolium chloride ([EMIm]Cl)

^{1}H NMR (300 MHz, Chloroform-*d*) δ 10.42 (s, 1H, f), 7.55 (dt, *J* = 7.2, 1.8 Hz, 2H, d, e), 4.34 (q, *J* = 7.4 Hz, 2H, c), 4.04 (s, 3H, b), 1.52 (t, *J* = 7.4 Hz, 3H, a).

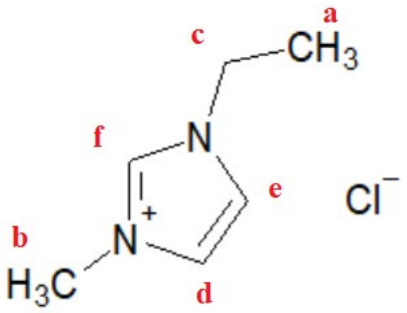

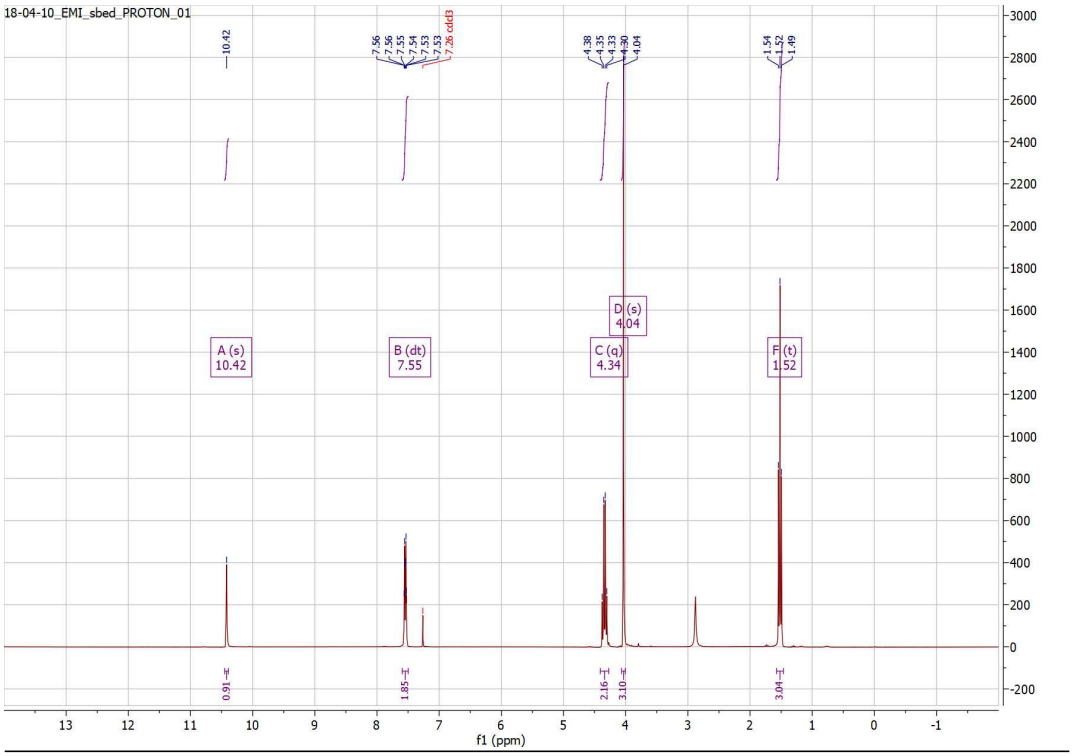

Figure S6. NMR spectrum of 1-ethyl-3-methylimidazolium choline ([EMIm]Cl)

Mixture of (*R*)-3-hydroxynonanoic and (*R*)-3-hydroxyheptanoic acids (HAs)

^{1}H NMR (300 MHz, Chloroform-*d*) δ 6.75 (br, 1H, OH) 4.03 (CH, b), 2.51 (m, CH_2, a), 1.6-1.2 (m, CH_2, c-g), 0.87 (m, CH_3, h)

Ref. Chem. Commun., 2011,47, 7812-7814

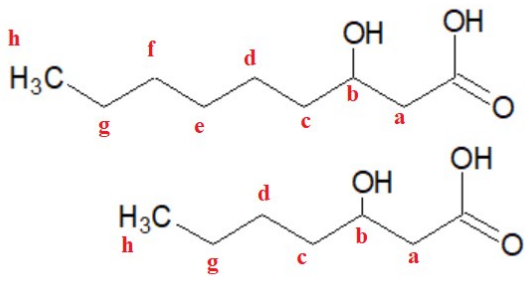

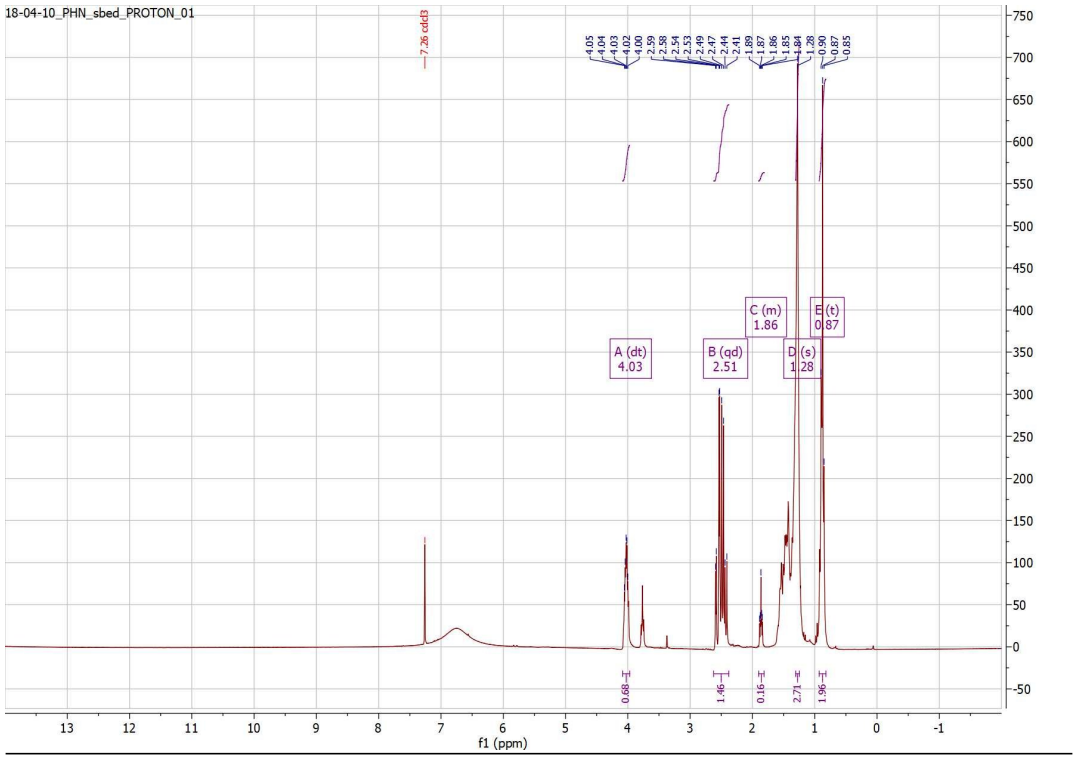

Figure S7. NMR spectrum of mixture of hydroxyacids (HAs)

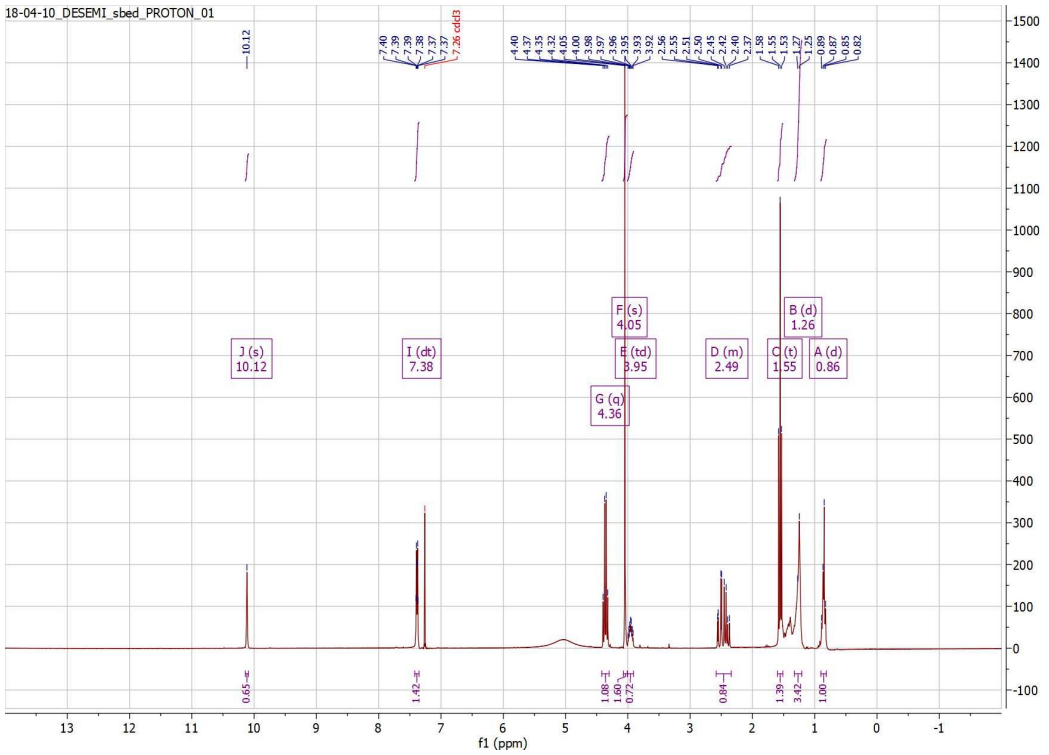

Figure S8. NMR spectrum of mixture of ([EMIm]Cl):Has

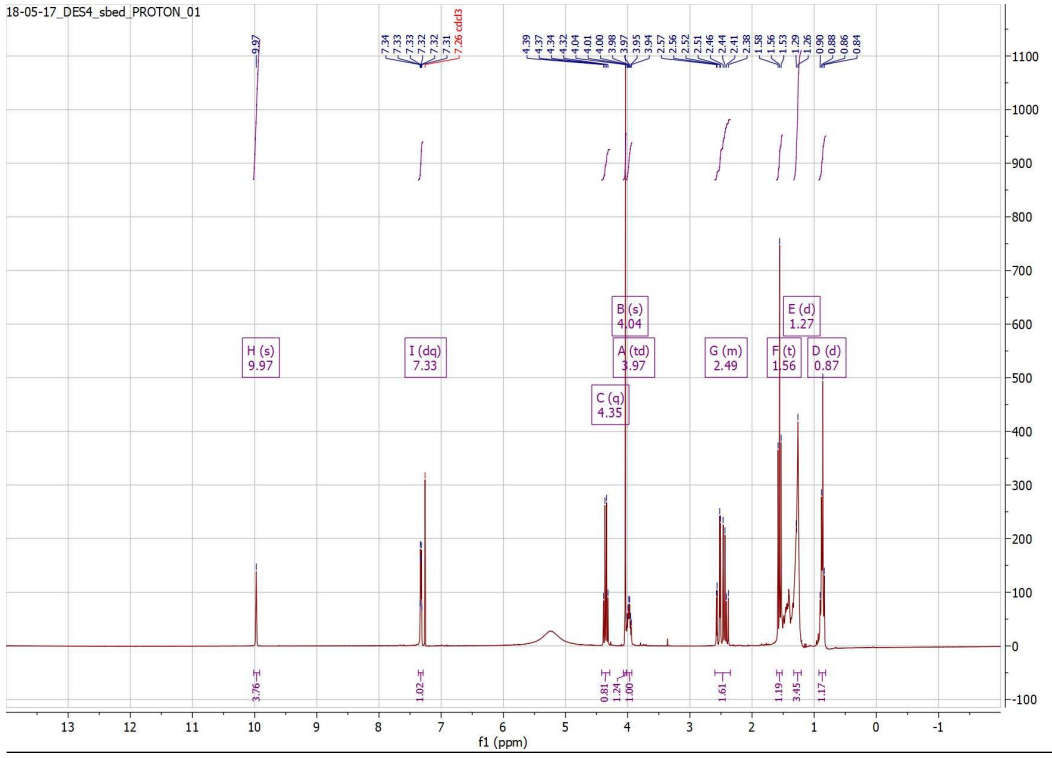

Figure S9. NMR spectrum of mixture of ([EMIm]Cl):2Has

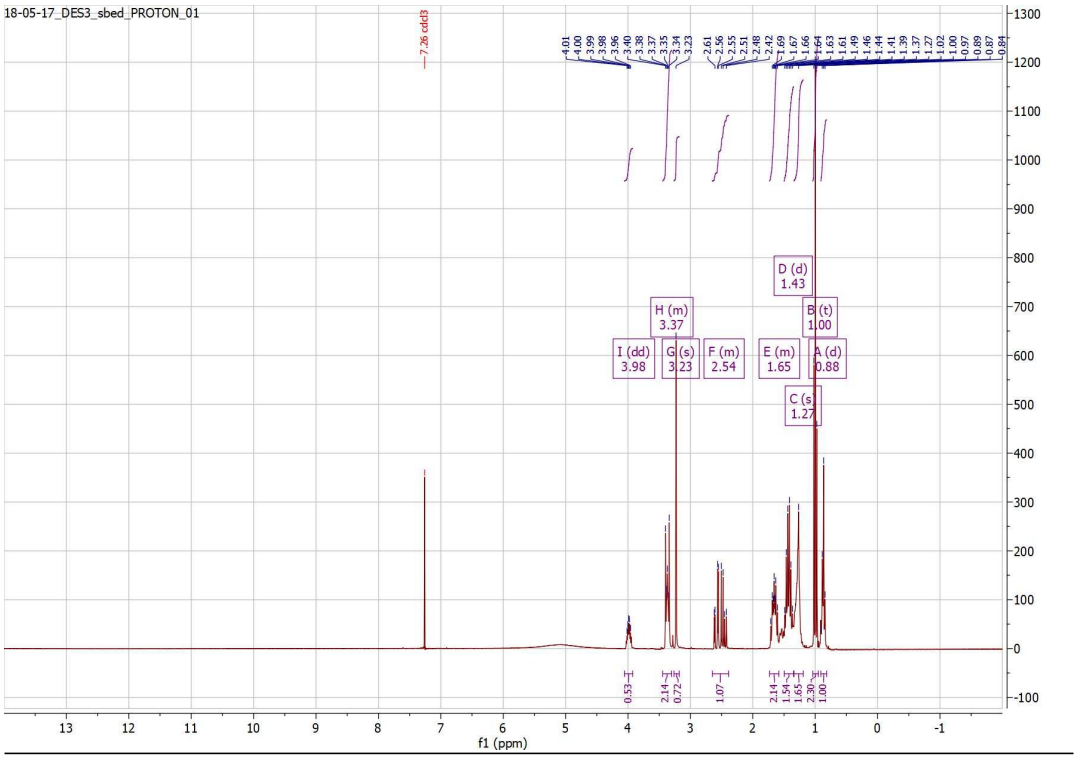

Figure S10. NMR spectrum of mixture of ([TBMA]Cl):Has

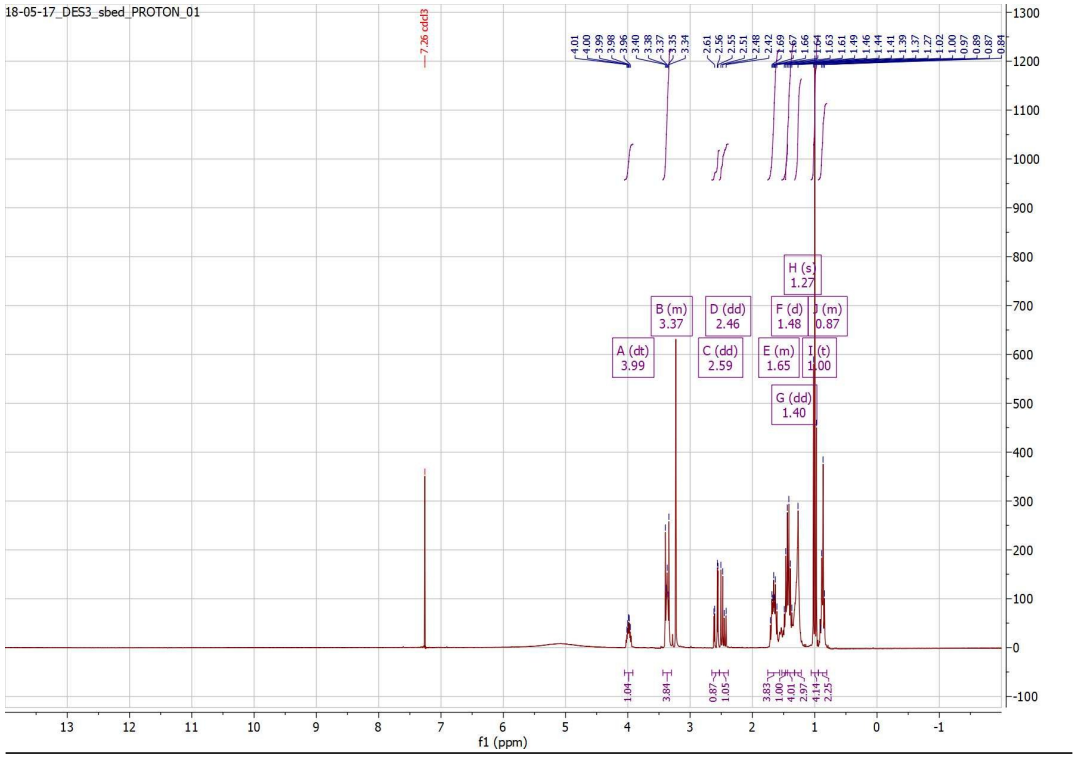

Figure S11. NMR spectrum of mixture of ([TBMA]Cl):2Has

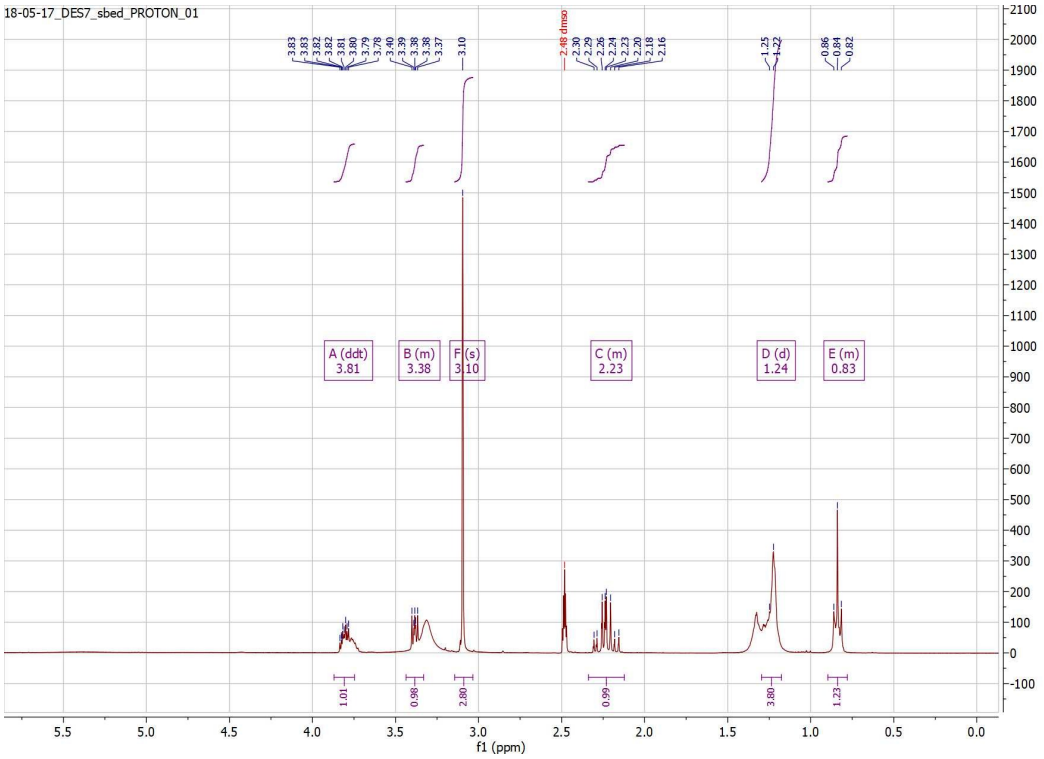

Figure S12. NMR spectrum of mixture of ([Ch]Cl):2Has

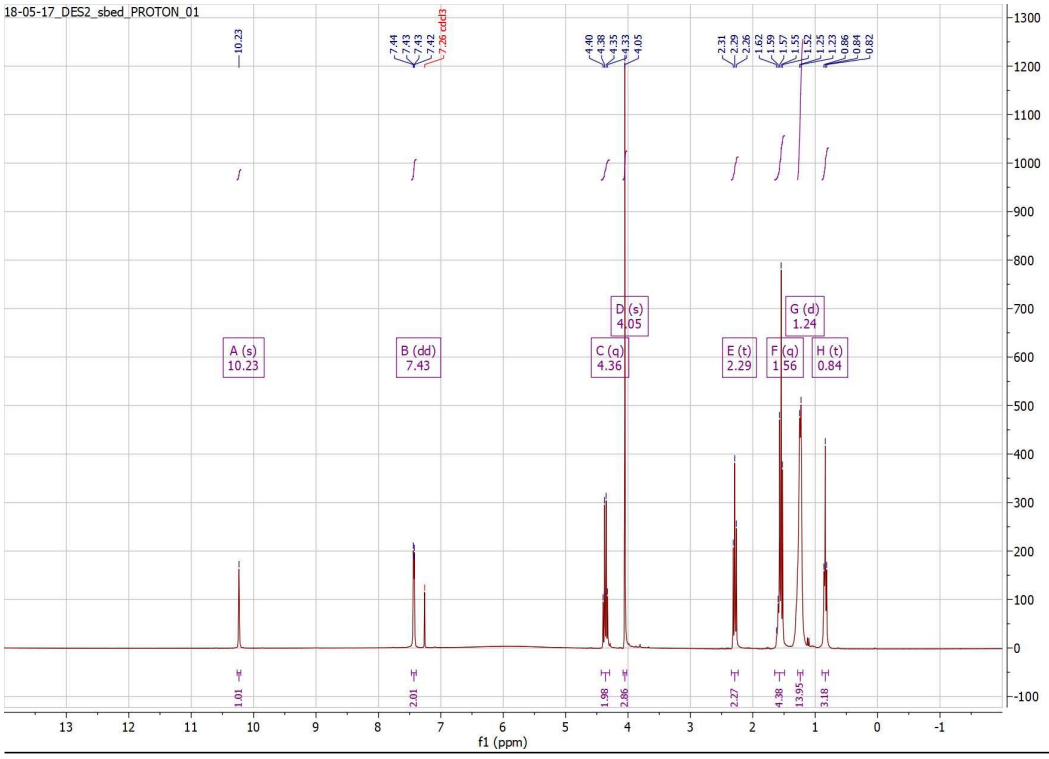

Figure S13. NMR spectrum of mixture of ([EMIm]Cl):Aliph

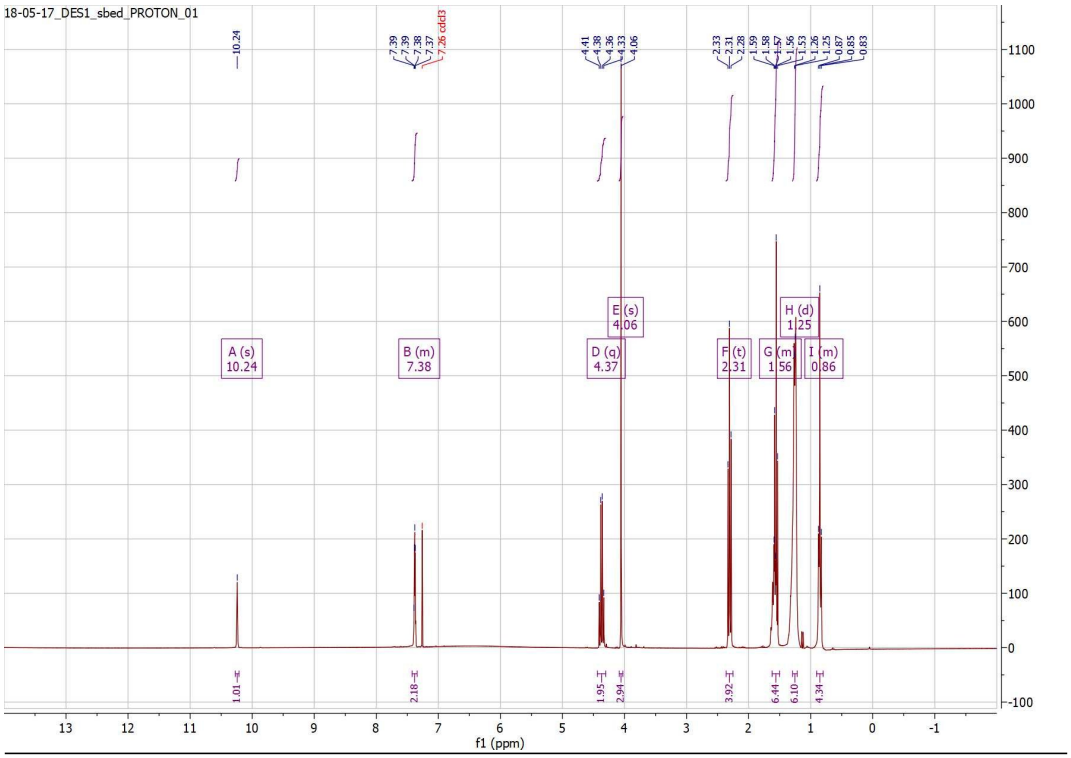

Figure S14. NMR spectrum of mixture of ([EMIm]Cl):2Aliph

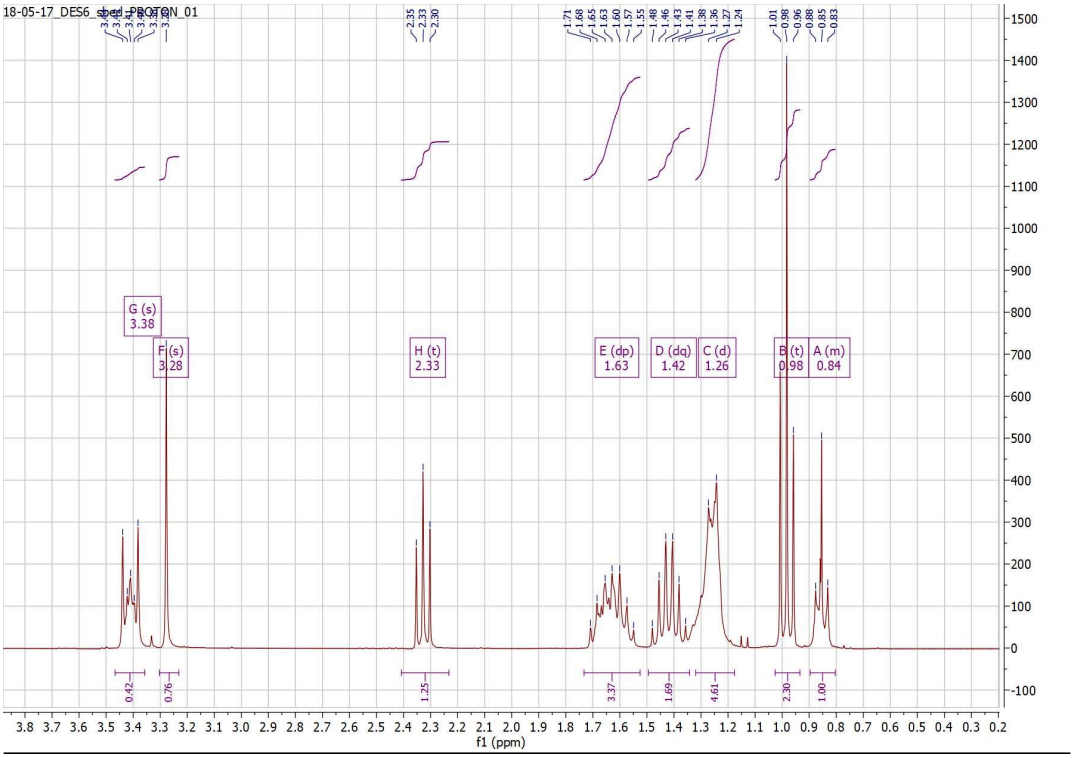

Figure S15. NMR spectrum of mixture of ([TBMA]Cl):Aliph

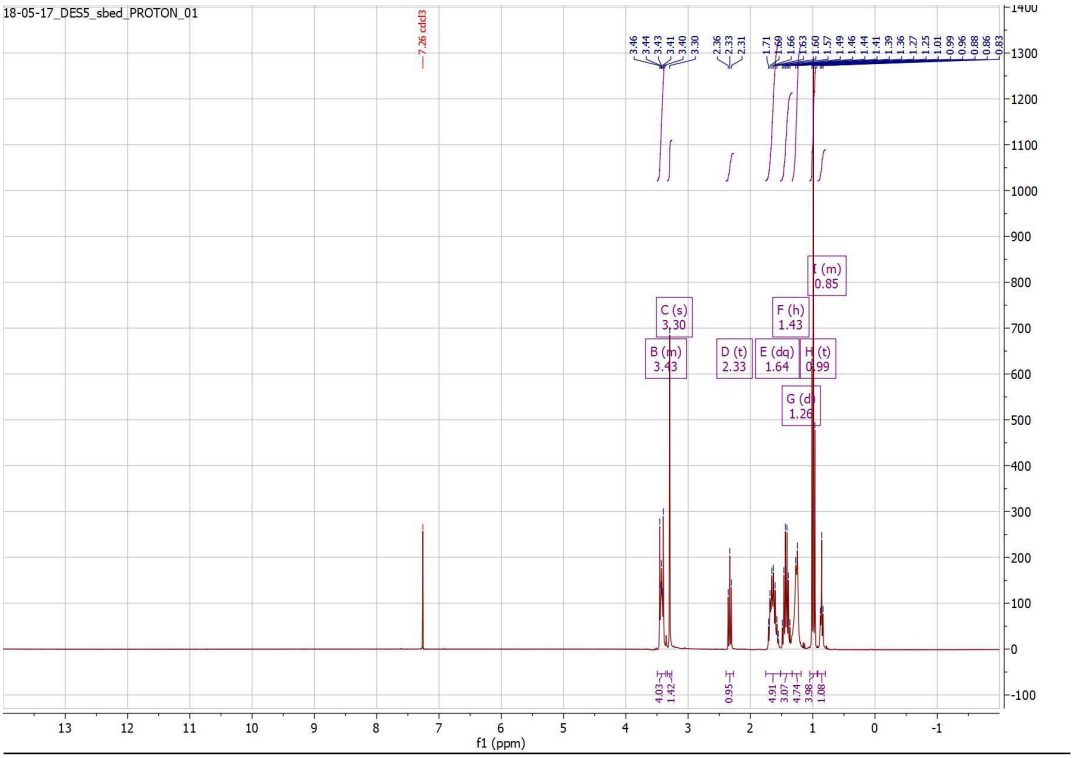

Figure S16. NMR spectrum of mixture of ([TBMA]Cl):2Aliph

IR spectra

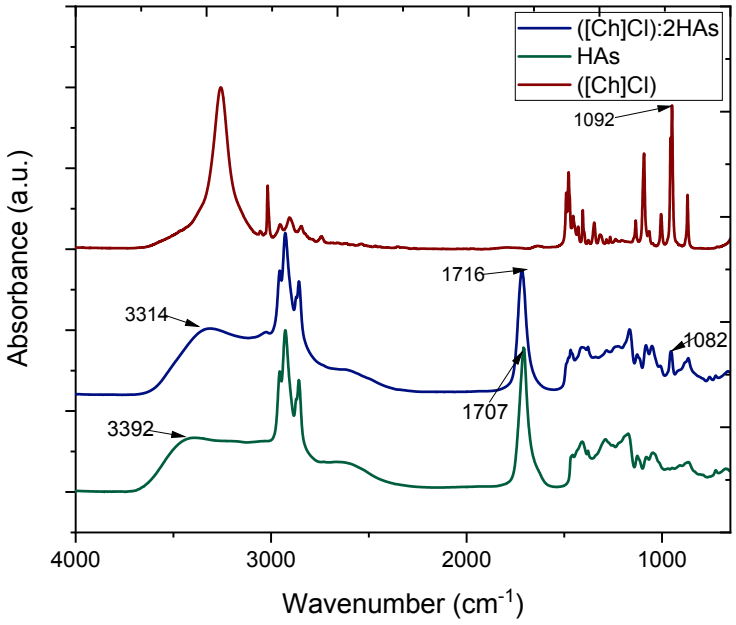

Figure S17. IR spectra of choline chloride ([Ch]Cl), mixture of hydroxyacids (Has) and ([TBMA]Cl):2HAs

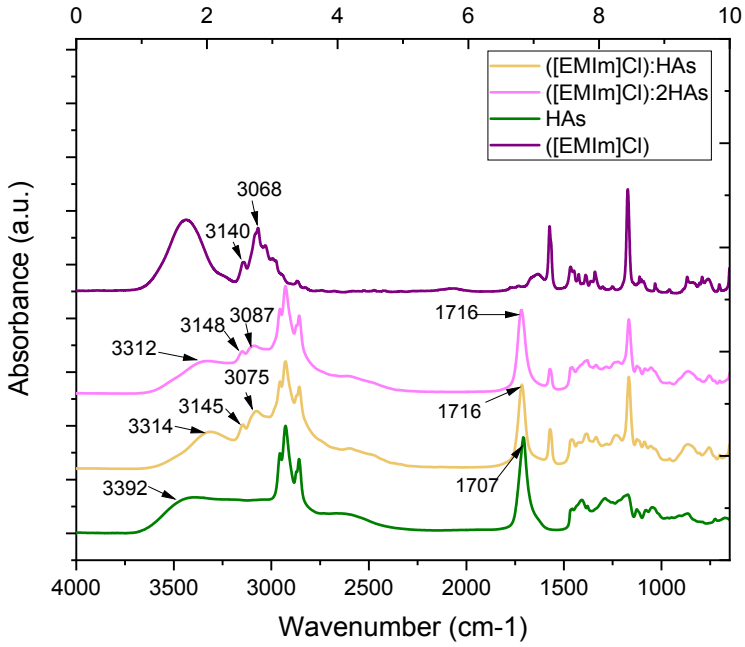

Figure S18. IR spectra of 1-ethyl-3-methylimidazolium chloride ([EMIm]Cl), mixture of hydroxyacids (HAs) and prepared DESs: ([EMIm]Cl):HAs and ([EMIm]Cl):2Has

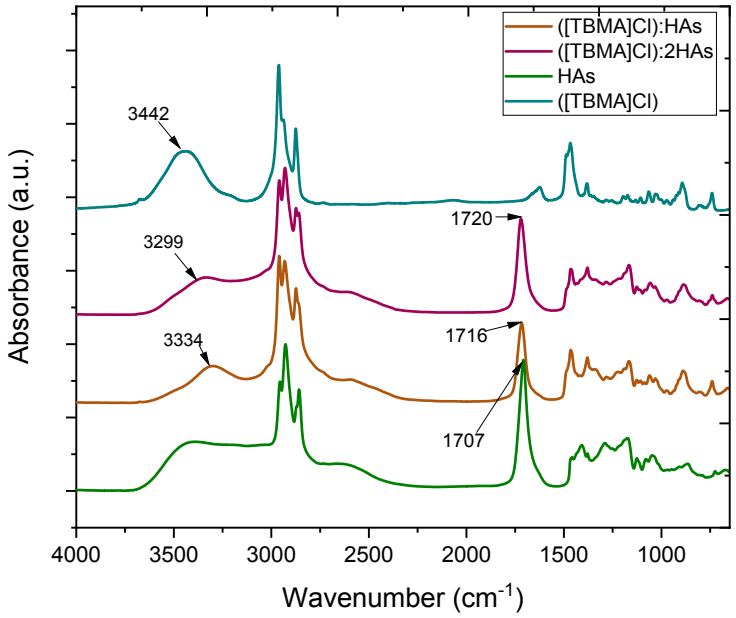

Figure S19. IR spectra of tributylmethylammonium chloride ([TBMA]Cl), mixture of hydroxyacids (HAs) and prepared DESs: ([TBMA]Cl):HAs and ([TBMA]Cl):2HAs

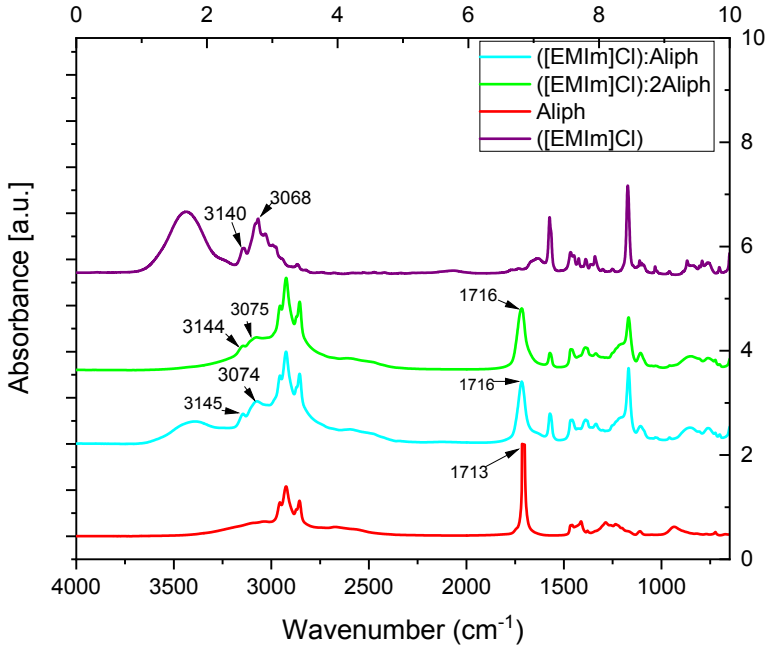

Figure S20. IR spectra of 1-ethyl-3-methylimidazolium chloride ([EMIm]Cl), mixture of alkanoic acids (Aliph) and prepared DESs: ([EMIm]Cl):Aliph and ([EMIm]Cl):2Aliph

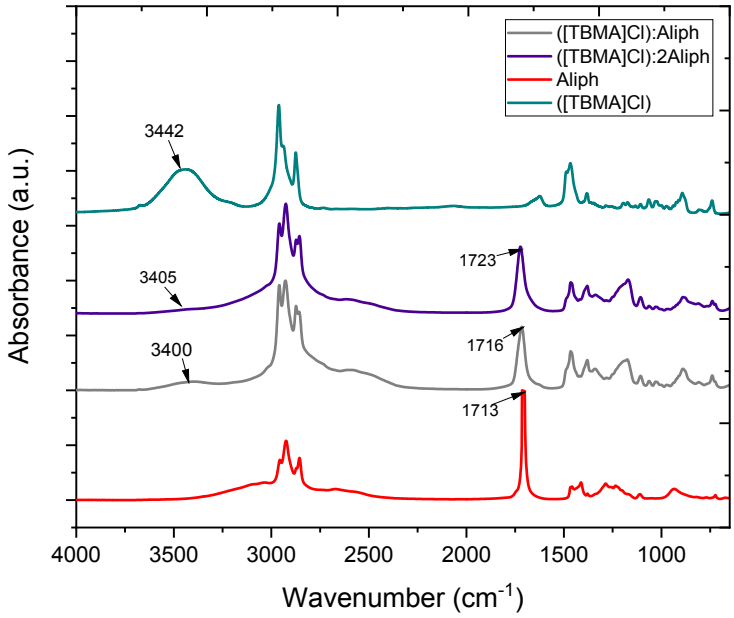

Figure S21. IR spectra of tributylmethylammonium chloride ([TBMA]Cl), mixture of alkanoic acids (Aliph) and prepared DESs: ([TBMA]Cl):Aliph and ([TBMA]Cl):2Aliph

Polarity of DESs

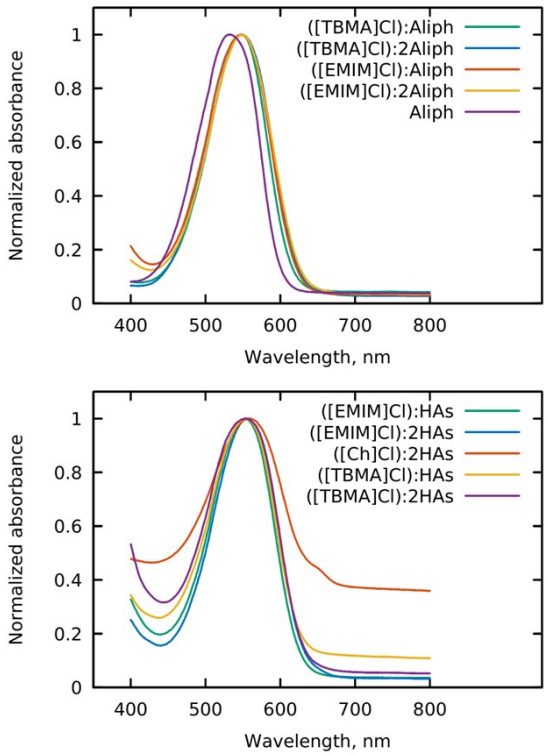

Fig. S22. UV-VIS spectra of Nile Red (~0.05mg mL^{-1}) dissolved in DESs

Table S1. Comparison of Nile Red Transition Energies ($E_{T(NR)}$) in DESs

DES	λ_{max}, nm	E_T(NR), kcal mol^{-1}
([TBMA]Cl):Aliph	549	52.1
([TBMA]Cl):2Aliph	548	52.2
([EMIm]Cl):Aliph	547	52.3
([EMIm]Cl):2Aliph	549	52.1
Aliph	532	53.7
([EMIm]Cl):HAs	553	51.7
([EMIm]Cl):2HAs	553	51.7
([Ch]Cl):2HAs	558	51.2
([TBMA]Cl):HAs	553	51.7
([TBMA]Cl):2HAs	552	51.8

DSC measurements

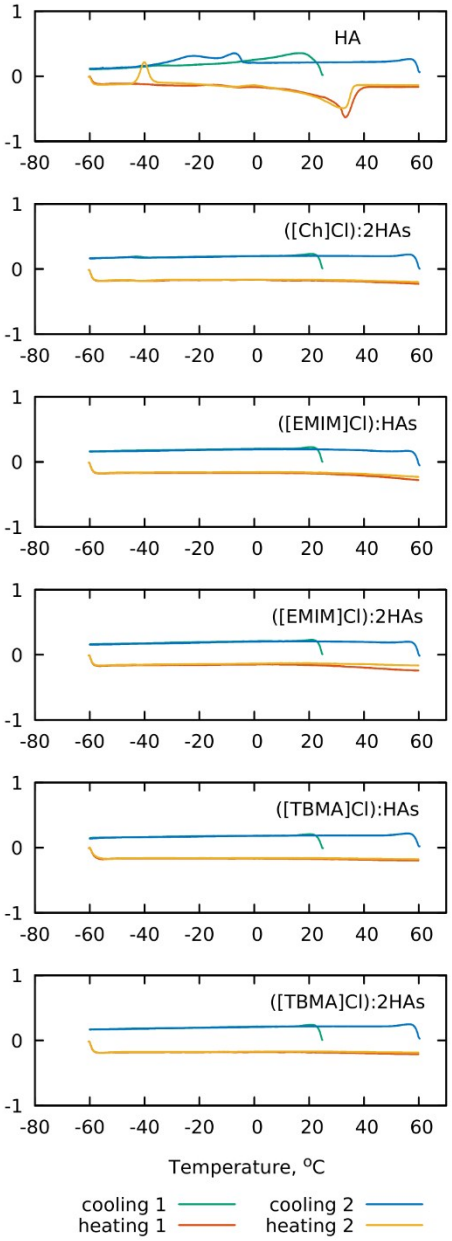

Figure S23. DSC thermograms showing the variation of the heat flow (mW/mg) with temperature (first and second run) for aliphatic and HAs based DESs (scan rate of 5°C/min, exo up).

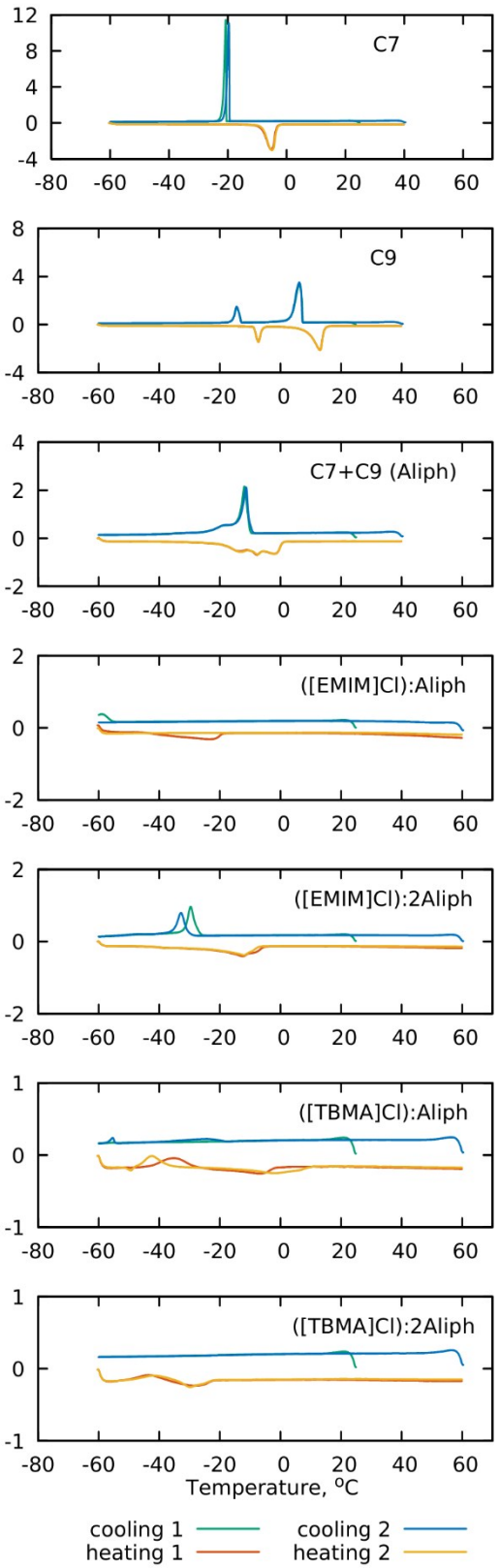

Figure S24. DSC thermograms showing the variation of the heat flow (mW/mg) with temperature (first and second run) for hydroxylic acids and carboxylic acids based DESs (scan rate of 5°C/min, exo up).

TGA/DTG results

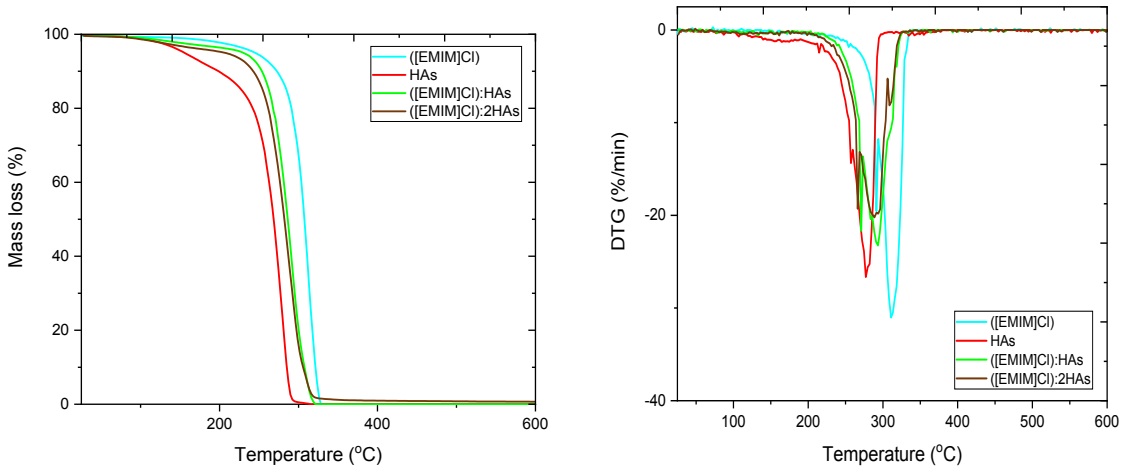

Figure S25. Thermal degradation (on the left) and DTG (on the right) curves of constructed 1-ethyl-3-methylimidazolium chloride based DESs – ([EMIm]Cl):HAs; ([EMIm]Cl):2HAs and its components: ([EMIm]Cl) and HAs

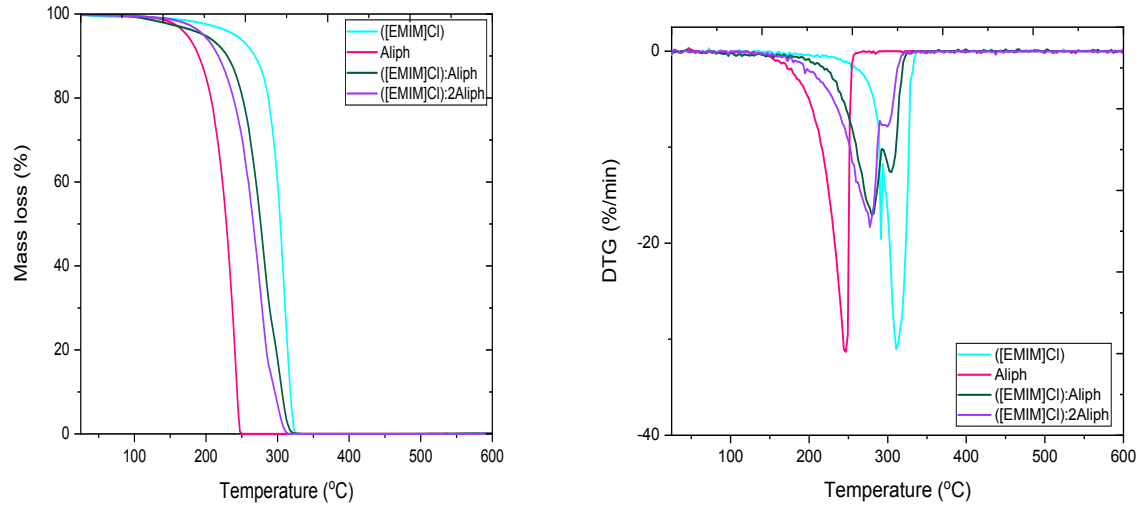

Figure S26. Thermal degradation (on the left) and DTG (on the right) curves of constructed 1-ethyl-3-methylimidazolium chloride based DESs – ([EMIm]Cl):Aliph; ([EMIm]Cl):2Aliph and its components: ([EMIm]Cl) and Aliph

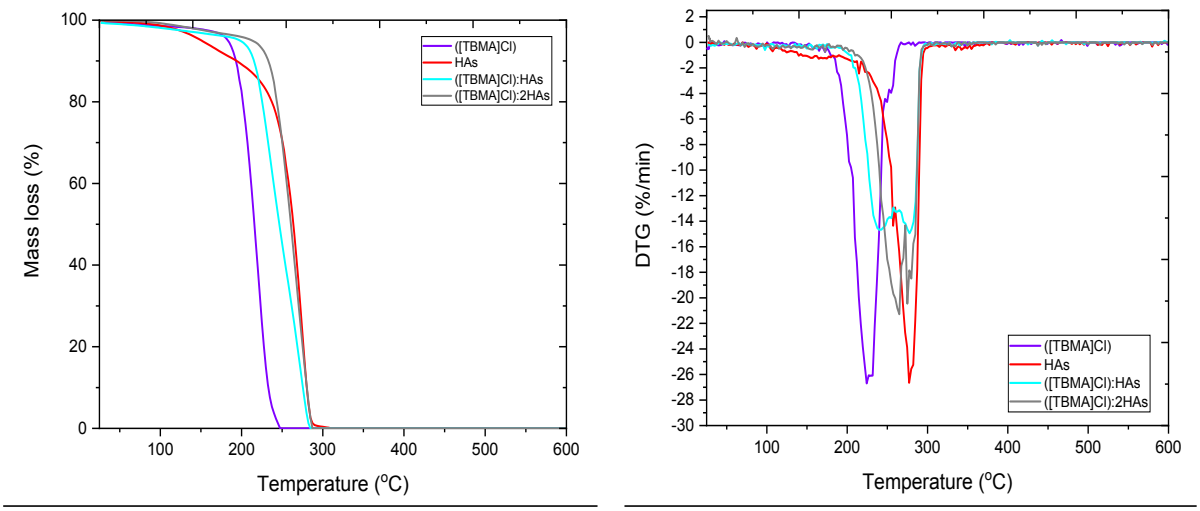

Figure S27. Thermal degradation (on the left) and DTG (on the right) curves of constructed tributylmethylammonium chloride based DESs – ([TBMA]Cl):HAs; ([TBMA]Cl):2HAs and its components: ([TBMA]Cl) and HAs

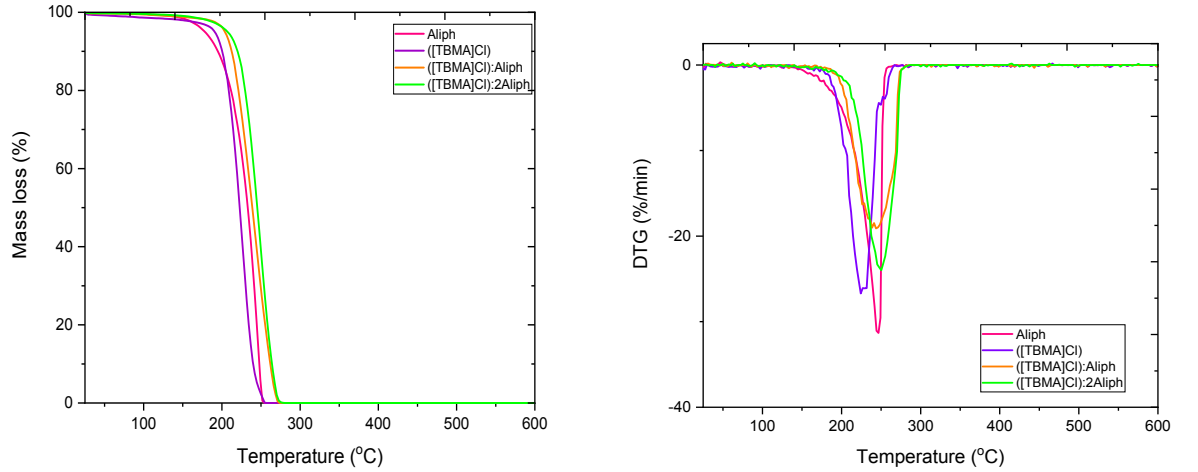

Figure S28. Thermal degradation (on the left) and DTG (on the right) curves of constructed tributylmethylammonium chloride based DESs – ([TBMA]Cl):Aliph; ([TBMA]Cl):2Aliph and its components: ([TBMA]Cl) and Aliph

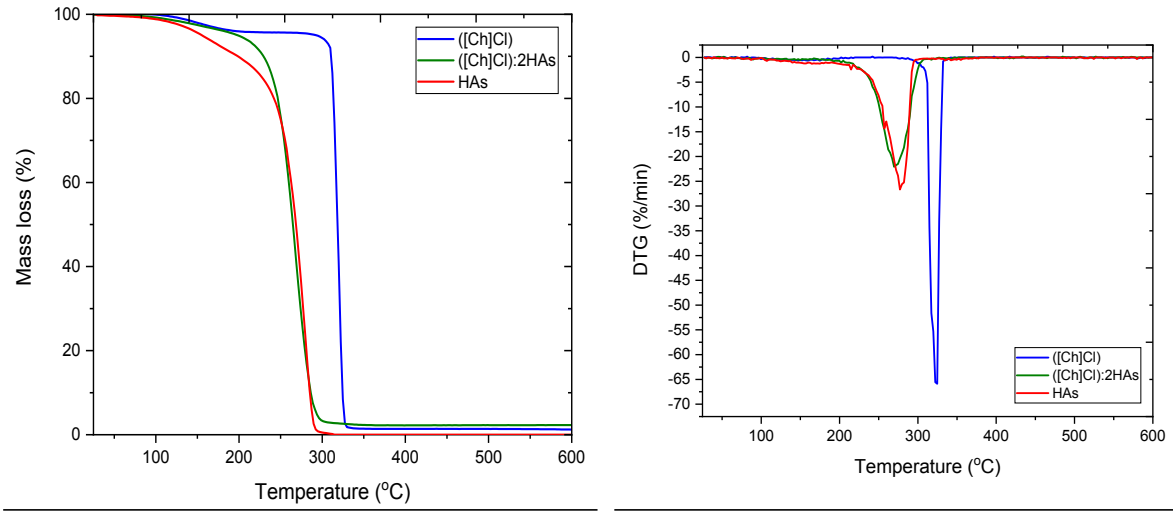

Figure S29. Thermal degradation (on the left) and DTG (on the right) curves of constructed choline chloride based DES – ([Ch]Cl):2HAs and its components: ([Ch]Cl) and HAs

Biodegradability of DESs

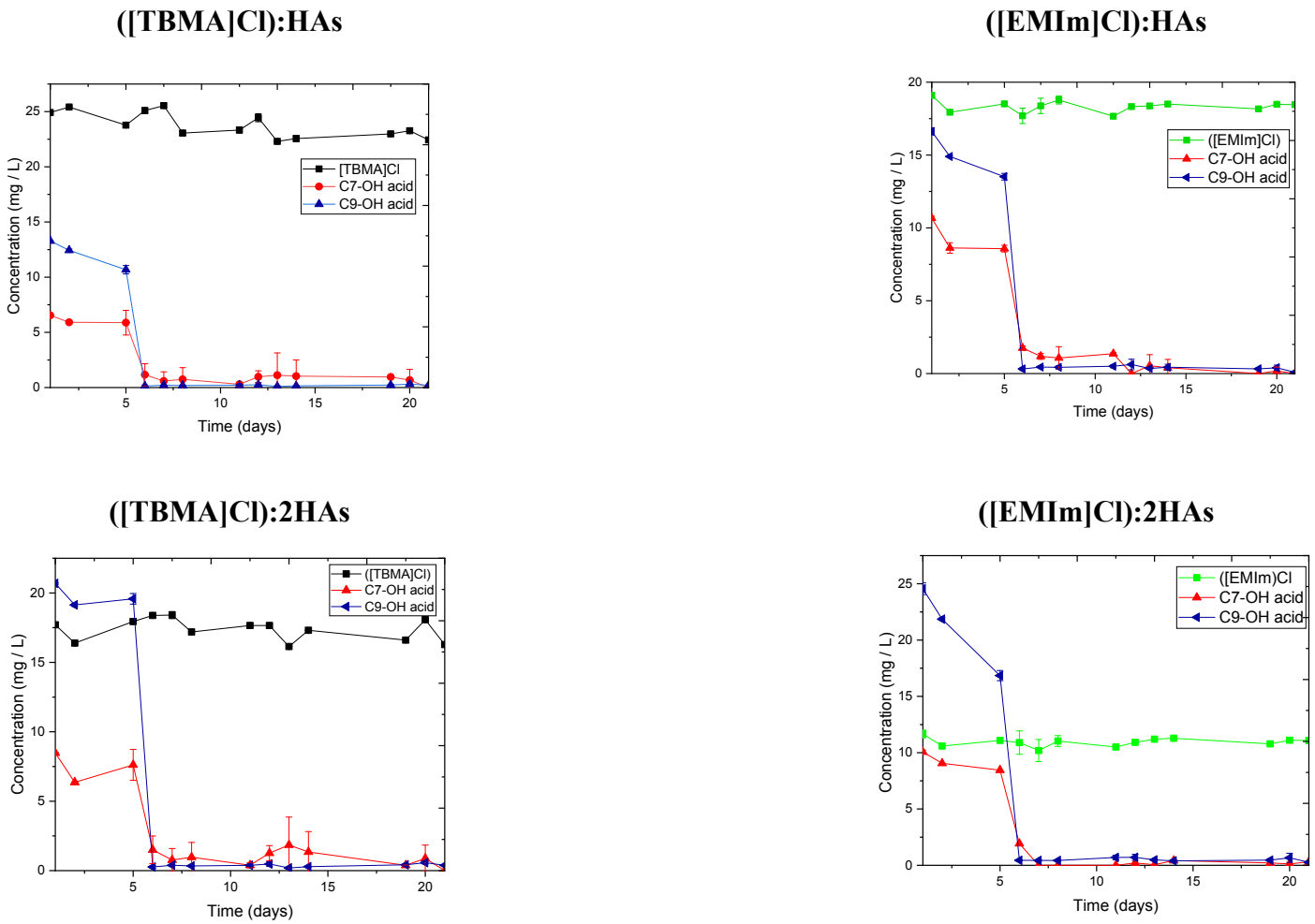

Figure S30. Biodegradation test of prepared hydroxyacids based DESs

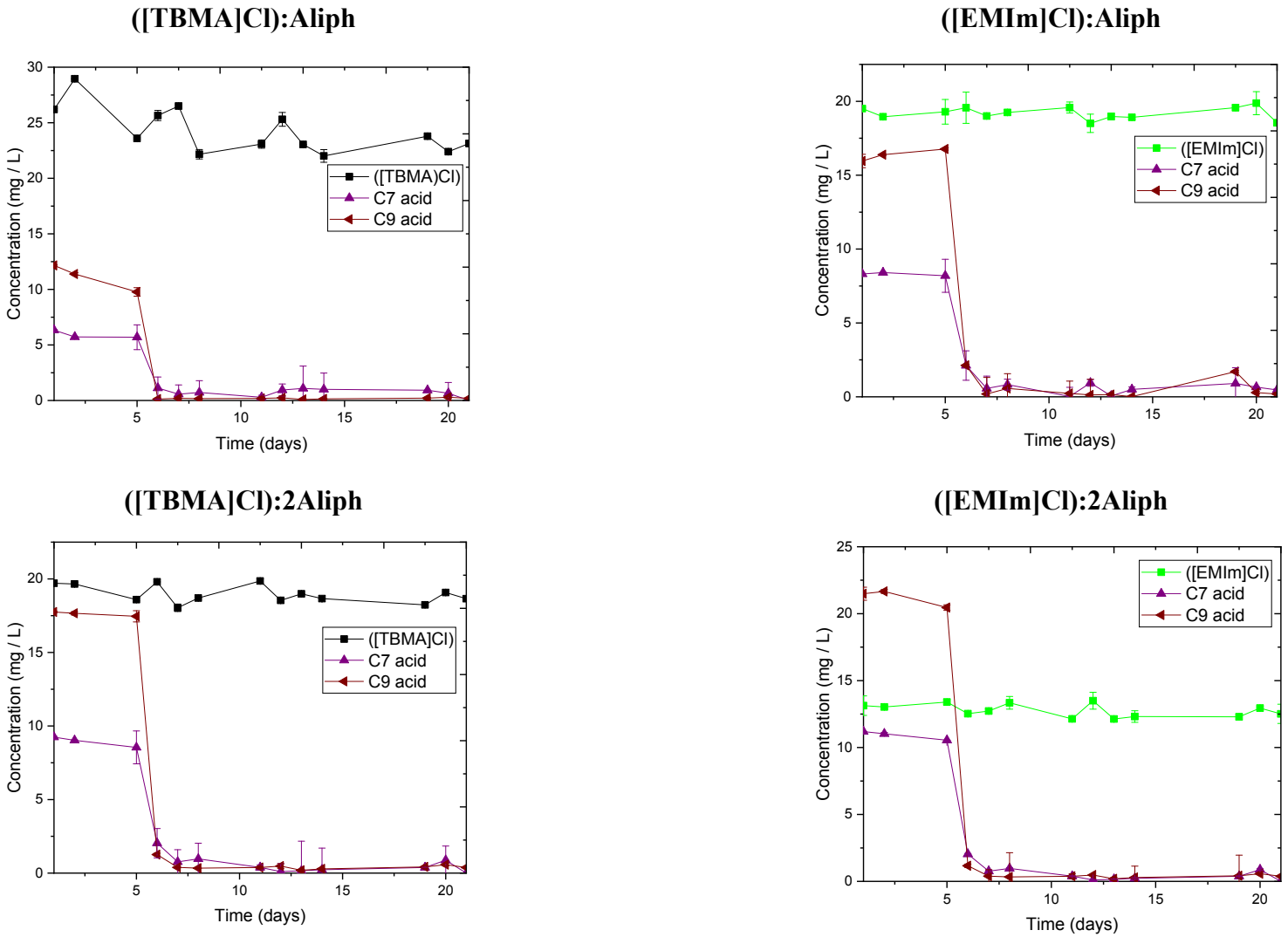

Figure S31. Biodegradation test of prepared aliphatic based DESs

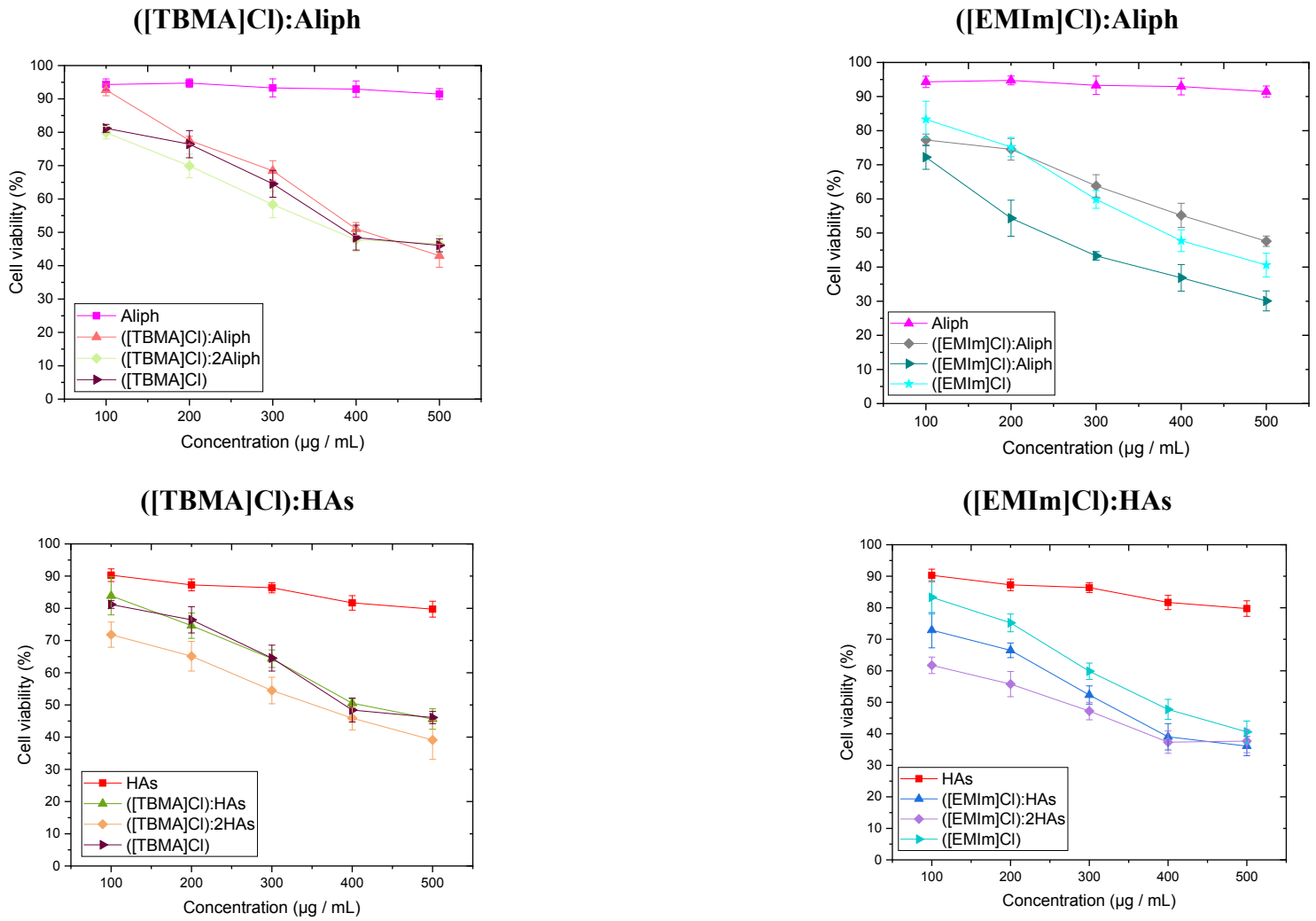

Figure S32. Cell viability of MEF 3T3 after 24h exposure to prepared aliphatic and hydroxyacid based DESs